Folding of a Monomeric Porin, OmpG, in Detergent Solution[†]

Sean Conlan[‡] and Hagan Bayley*[,‡,§]

Department of Medical Biochemistry and Genetics, The Texas A&M University System Health Science Center, College Station, Texas 77843-1114, and Department of Chemistry, Texas A&M University, College Station, Texas 77843-3255

Received March 17, 2003; Revised Manuscript Received June 3, 2003

ABSTRACT: OmpG, a porin from *E. coli*, has been examined in planar lipid bilayers and in detergent solution. First, bilayer recordings were used to reinforce the evidence that the functional form of OmpG is a monomer. Both pH-dependent gating and blockade by covalent modification add support to this proposal. The findings contrast with the properties of the classical porins, which function as trimers. Second, the folding of OmpG in detergent solution was examined. A water-soluble form of OmpG was obtained by dialysis from denaturant into buffer. Incubation of water-soluble OmpG in detergent results in conversion to a form that possesses the hallmarks of a β barrel. The folding of water-soluble OmpG in detergent was monitored by circular dichroism, protease resistance, and heat modifiability. OmpG is first transformed into an intermediate with increased β-sheet content on the time scale of minutes at 23 °C. This is followed by the slow acquisition of heat modifiability and protease resistance over several hours. The formation of a β barrel during this period was demonstrated in a double cysteine mutant by using intramolecular disulfide bond formation to report N and C terminus proximity. Finally, conditions are presented for folding OmpG with greater than 90% efficiency, thereby paving the way for structural studies.

Gram-negative bacteria are surrounded by a double membrane structure. The outer membrane serves as a semipermeable barrier, allowing nutrients to penetrate the cell and preventing noxious substances from entering (*1*). The permeability of the barrier is controlled by a set of outer membrane proteins, the majority of which are porins (*2*−*5*). Nonspecific porins, like OmpF and OmpC, allow small molecules (<600 Da) access to the periplasm. Other porins, LamB for instance, transport specific solutes, in this case maltodextrins.

The porin OmpG was found in a screen for *Escherichia coli* with increased outer membrane permeability (*6*). OmpG is able to rescue the growth of porin-deficient bacteria on media containing maltodextrins as large as maltopentose as the sole carbon source. The gene for OmpG encodes a 301 amino acid polypeptide, which is processed during export by removal of a 21-amino acid leader sequence to yield the mature protein. The physiological role of OmpG is not clear. OmpG is not detected in the outer membrane of several *E. coli* strains (*E. coli* K12 strains 679, Y10, W1, and AB1157, *E. coli* B, *E. coli* C, and *E. coli* K1) by western blot analysis. Despite this, the gene for OmpG gene is detected by PCR[1] analysis in the genomes of these bacteria, indicating that the lack of expression may be due to the growth conditions.

The *E. coli* strains RAM123 and RAM194 express OmpG due to a deletion upstream of the gene that places it under the control of the *pspA* (phage shock protein) promoter (*7*). OmpG transcripts were not seen in the parent strain, DME553, by northern blot analysis. OmpG can be extracted from outer membrane fractions of RAM123 or RAM194 cells by solubilization in detergent. The extracted protein has an apparent molecular weight of 28 kDa when analyzed by SDS-PAGE without heating. Heating the extracted protein results in a change in the apparent molecular weight to 32 kDa, a phenomenon known as heat modifiability. This property is seen in other outer membrane proteins (OMPs), including OmpA (*8*) and PhoE (*9*). All outer membrane proteins studied to date are β barrels, and one possible explanation for heat modifiability is the stability imparted by the extensive hydrogen-bond network that holds β barrels together. Heat modifiability is often used as a criterion for the folding or refolding of outer membrane proteins, such as OmpA (*10, 11*).

The in vitro channel-forming properties of OmpG have been investigated. A liposome swelling assay demonstrated that OmpG forms a pore capable of transporting large solutes (*7*). In these assays, dextran-filled proteoliposomes were made by using OmpG extracted from the outer membrane. The liposomes were then diluted into isosmotic solutions of different sized sugars. The permeation rates of the sugars

[†] This work was supported by the DOE and NIH.

* Corresponding author. E-mail: bayley@tamu.edu. Tel: (979) 845-7047. Fax: (979) 847-9481.

[‡] The Texas A&M University System Health Science Center.

[§] Texas A&M University.

[1] Abbreviations: ANS, 8-anilino-1-naphthalene sulfonate; CD, circular dichroism; DEAE, diethylaminoethyl-; DTT, dithiothreitol; EDTA, ethylenediaminetetraacetic acid; LB medium, Luria Bertani medium; MePEG-OPSS, monomethoxypoly(ethylene glycol) *o*-pyridyl disulfide; MES, 2-[*N*-morpholino]ethanesulfonic acid; MRE, mean residue ellipticity; NEM, *N*-ethylmaleimide; OG, *n*-octyl-β-D-glucopyranoside; OMP, outer membrane protein; SDS, sodium dodecyl sulfate; SDS-PAGE, SDS polyacrylamide gel electrophoresis; Tris, tris(hydroxymethyl)aminomethane; PCR, polymerase chain reaction; PMSF, phenylmethylsulfonylfluoride.

10.1021/bi0344228 CCC: $25.00
Published on Web 07/16/2003

through OmpG were determined from changes in the light scattering of the proteoliposome suspension produced by osmotic swelling. Correlation of the permeation rates with the molecular weights of the sugars gave an estimated pore diameter of 20 Å for OmpG (*7*).

All of the classical porins (e.g., OmpF, OmpC, PhoE, LamB) function as trimers. These complexes are stable; for example, OmpF can be extracted from the outer membrane of *E. coli* as an SDS-resistant trimer (*12*). In addition, OmpF has been crystallized as a trimer (*13*), and the structure is consistent with images from electron microscopy (*14*) and atomic force microscopy (*15*, *16*). In contrast, OmpG appears to function as a monomer. Oligomeric forms have not been detected on gels before or after chemical cross-linking (*7*). Furthermore, OmpG exhibits characteristics of a functional monomer in planar bilayers (*17*). The single channel conductance of OmpG is 0.81 nS in 1 M NaCl, which is comparable to the 0.5−1 nS conductance normally seen for each monomer of a trimeric porin under similar conditions. OmpG closes in a single step in response to an elevated transmembrane potential (*17*), instead of the three steps normally seen with trimeric porins (*18*−*21*). Finally, the binding of the trivalent cation gadolinium (Gd^{3+}) is consistent with a monomer. OmpG binds Gd^{3+} with a Hill coefficient of 1.37 at +40 mV and 1.39 at −40 mV, indicating a single binding site. In contrast, OmpF binds Gd^{3+} with a Hill coefficient of 3.51 at +40 mV and 5.35 at −40 mV, indicating multiple cooperative binding sites (*17*). A high-resolution crystal structure does not exist for OmpG but two structural models have been proposed, one predicting 16 transmembrane strands (*7*) and another predicting 14 transmembrane strands (*17*). In addition to the predictions, a two-dimensional projection structure has been obtained at 6 Å by electron diffraction (*22*). This structure shows a monomeric, roughly circular molecule, 25 Å in diameter, which the authors argue is consistent with a 14-stranded β barrel.

OmpG is a promising candidate for use as a scaffold for engineering pores with new functions. There has been considerable success in engineering the heptameric β-barrel pore-forming toxin, α-hemolysin (*23*−*27*), and effort is also being put into trimeric porins (*28*−*31*). Despite this, there are difficulties in engineering pores that are composed of multiple subunits. For example, a point mutation in the α-hemolysin monomer is repeated seven times in the assembled pore, and therefore special methods were developed for obtaining heteroheptamers (*27*, *32*, *33*). A porin like OmpF is also problematic, since even though mutations occur once per pore, the functional unit contains three such mutant pores. A monomeric porin offers an advantage over these multimeric pores because a single polypeptide encodes a single functional pore. In the present work, additional experiments on OmpG were performed with the goal of establishing the pore as a viable platform for protein engineering. The new work confirms the monomeric state of OmpG. Furthermore, the folded forms and folding intermediates of OmpG were dissected by using a variety of biochemical and spectroscopic techniques. Conditions are presented for folding OmpG in vitro with >90% efficiency. Knowledge about the folding pathway is an important addition to the limited information available on membrane protein folding. The conditions for optimal folding presented here pave the way for structural studies on OmpG.

MATERIALS AND METHODS

Chemicals. Genapol X-080 detergent was from Fluka (Milwaukee, WI). *n*-Octyl-β-D-glucopyranoside (OG) was from Calbiochem (La Jolla, CA) or Anatrace (Maumee, OH). Proteinase K was from Invitrogen (Carlsbad, CA). Monomethoxypoly(ethylene glycol) *o*-pyridyl disulfide, M_r 970 Da (MePEG-OPSS), was synthesized by Shearwater Polymers (Huntsville, AL). The thiol-directed dye Alexa 594 C_5 maleimide was from Molecular Probes (Eugene, OR). DEAE-Sepharose was from Amersham Pharmacia Biotech (Piscataway, NJ). Precast SDS-PAGE gels (PAGEr Gold) were from Cambrex (East Rutherford, NJ). Unless otherwise noted, additional reagents were from Sigma (St. Louis, MO).

Cloning and Strains. The cloning of a gene for mature OmpG (OmpGm) into the pT7-SMC vector (*34*) has been described previously (*17*). OmpGm with a cysteine at position 93 (Gm93C) was made by using in vivo recombination PCR (*35*) with two mutagenic primers (forward, 5′-GAG CTG TGT GTG CAT TAT CAG; reverse, 5′-CAC ACA CAG CTC CGG GCG ATC) and two nonmutagenic primers (SC46, 5′-ATA AAG TTG CAG GAC CAC TTC TG; SC47, 5′-CAG AAG TGG TCC TGC AAC TTT AT). The sequence of the OmpG gene in the resulting construct, pT7-Gm93C, was determined and found to match the expected sequence. The double cysteine mutant (Gm2C) was made by amplifying pT7-OmpGm with two mutagenic primers (forward, 5′-TAG TAA TAG TAA CAT ATG TGC GAG GAA AGG AAC GAC TGG; reverse, 5′-CTA CTA AAG CTT TTA GAA GCA GTA ATT TAC GCC GAC ACC). The new gene encodes a cysteine following the N-terminal methionine and a serine-to-cysteine mutation at the penultimate codon. The addition of the N-terminal cysteine results in a protein that is two residues longer (Met-Cys-) than the wild-type protein processed by leader peptidase. The PCR product was cloned into the Topo-TA plasmid (Invitrogen, Carlsbad, CA). The insert was then removed by digestion with NdeI and HindIII and ligated into the expression vector, pT7-SMC (*34*), which had been digested with the same enzymes. The sequence of the insert in pT7-SMC was determined and matched the expected sequence. All cloning was carried out in *E. coli* XL-10 Gold cells (Stratagene, La Jolla, CA). Protein expression was carried out in porin-deficient *E. coli* PC2889 cells [BL21(DE3)ΔlamB ompR] from the Netherlands Culture Collection (Utrecht, Netherlands). The cells were transformed with the pLysE plasmid, which confers chloramphenicol resistance for tight control of expression from the T7 promoter (*36*), and designated PC2889E.

Expression and Purification. OmpGm and the cysteine mutants were expressed and purified by similar procedures. For example, to obtain OmpGm, a starter culture of PC2889E cells, transformed with the pT7-OmpGm plasmid, was grown at 37 °C in LB medium (10 mL) containing chloramphenicol (20 μg/mL) and ampicillin (50 μg/mL). This culture was used to inoculate LB medium (1.6 L) containing ampicillin (50 μg/mL). After the OD_{600} reached a value of 0.7, expression of OmpGm was induced with 0.5 mM isopropyl-β-D-thiogalactoside. The cells were grown for a further 3 h at 37 °C and then recovered by centrifugation and frozen. The cell pellet was cracked with lysis buffer (10 mL: 200 μg/mL hen egg white lysozyme, 1 mM phenylmethylsulfonylfluoride

(PMSF), 10 mM Tris·HCl, 1 mM EDTA, pH 8.0) on ice for 15 min. The viscosity of the lysate was reduced by incubation with 50 μg/mL DNaseI and 2 mM $MgCl_2$, for 5 min on ice. The lysate was then centrifuged at 60 000*g* in a TL100.2 rotor with a Beckman TL-100 ultracentrifuge. The resulting insoluble fraction was washed twice in 10 mM Tris·HCl, pH 8.0, 1 M urea (10 mL). The pellet was then dissolved in fresh denaturation buffer (50 mL: 8 M urea, 10 mM Tris·HCl, pH 8.0) with rocking and loaded onto a DEAE-Sepharose column (12.5 mL bed), which had been equilibrated with denaturation buffer. The bound protein was eluted with a linear gradient of NaCl (200 mL, 0−400 mM) in denaturation buffer. The fractions containing the protein were pooled (~30 mL) and dialyzed for 8 h at 4 °C against 10 mM Tris·HCl, pH 8.0 (2 L), with one buffer change. The protein concentration was determined by measuring the absorbance at 280 nm and using an extinction coefficient of 84 950 M^{-1} cm^{-1} (*37*). The purification yielded 10−50 mg of protein per liter of cells. Protein was stored frozen in aliquots at −80 °C. For proteins containing cysteine residues, 1 mM dithiothreitol (DTT) was present at all steps of a purification, and the protein was dialyzed into buffer containing 100 μM DTT for storage.

Reduction and Oxidation of Cysteine-Containing Proteins. Protein (1−3 mg/mL in 10 mM Tris·HCl, pH 8.0, 100 μM DTT) was reduced with additional DTT (20 mM final) and incubation at room temperature for 45 min. Complete reduction was confirmed by the absence of oxidized species by SDS-PAGE. For experiments where reductant would interfere with subsequent reactions, DTT was removed by gel filtration on a D-Salt column (Pierce, Rockford, IL). Applied volumes did not exceed 200 μL for a 7 × 50 mm column. The concentration of the eluted protein was typically ~50 μM.

Cysteine mutants were oxidized by the addition of excess Cu^{2+}(*o*-phenanthroline)$_2$. The oxidant was made by mixing *o*-phenanthroline and $CuSO_4$ in solution at a molar ratio of 3.6:1. The final concentration of copper in the oxidation reaction was 1.3 mM. The reaction was allowed to proceed for 5 min at 23 °C and then stopped by the addition of 5 mM (final) EDTA followed by 10 mM (final) *N*-ethylmaleimide (NEM), which was added to block any remaining free cysteines. Longer oxidation times (up to 45 min) did not result in additional oxidation as determined by SDS-PAGE.

Detergent CMC Determination Using ANS. The dye 8-anilino-1-naphthalene sulfonate (ANS) has greatly enhanced fluorescence in hydrophobic environments and can be used to determine the critical micelle concentration (CMC) of a detergent (*38*). The CMC is defined as the detergent concentration above which micelles are formed. A dilution series of detergent was made in a 96-well plate such that the dilutions spanned the expected CMC. The detergent was then mixed with 100 μM ANS (final), and the fluorescence was measured after 1 h in a Fluostar fluorescence plate reader (BMG Lab Technologies, Offenburg, Germany) using a 360 nm excitation filter and a 480 nm emission filter. Fluorescence intensity was plotted versus the final detergent concentration, and the CMC was determined from the breakpoint of the curve. Values measured for OG alone were in good agreement with published values (18−20 mM). The CMC of OG in the presence of 1.5 M urea was obtained in the same way. The CMC for the mixture of OG and 0.2% SDS (CMC 2.6 mM) could not be determined due to the absence of a clear breakpoint, but it appeared to be lower than the value for OG alone.

ANS Binding by OmpGm. ANS binding by OmpGm was measured in the presence of urea (0−4 M). Water-soluble OmpGm was mixed with several dilutions of urea in the presence of 100 μM ANS (final). The fluorescence was measured as described above using a plate reader.

Tryptophan Fluorescence Measurements. Fluorescence measurements were carried out with an SLM-AMINCO 8100 Series 2 Spectrofluorometer (Thermo Spectronic, Rockford, IL). The slit widths used for all experiments were 4 nm excitation and 4 nm emission. Tryptophans were excited at 300 nm to minimize the excitation of the 22 tyrosines in the protein. Data were collected in photon-counting mode with an integration time of 1 s. The data were corrected by subtracting the appropriate blank value and applying the instrument correction for the wavelength-dependent instrument response.

Gel Filtration. Gel filtration chromatography was performed on an ÄKTA Purifier liquid chromatography system equipped with a Superdex 200 HR 10/30 column (Amersham Pharmacia Biotech, Piscataway, NJ). The column was equilibrated with two column volumes of buffer (10 mM Tris·HCl, pH 8.0, 100 mM NaCl or 10 mM sodium phosphate, pH 8.0, 100 mM NaCl, 1% OG). The protein sample (100 μL) was applied and eluted in equilibration buffer. The absorption of the eluate was followed at 280 nm.

Circular Dichroism. CD spectra were acquired on an Aviv 62DS circular dichroism spectrometer (Lakewood, NJ) with a 10 mm-path length quartz cuvette. Samples were diluted into buffer (10 mM sodium phosphate, pH 8.0) with or without detergent. Spectra were corrected by subtracting the spectrum of buffer alone and converted to mean residue ellipticity (MRE) using the equation:

$$[\Theta] = (100m^\circ)/([\mathrm{prot}]_{\mathrm{mM}} l_{\mathrm{cm}} n)$$

where $[\Theta]$ is the MRE in deg cm^2 $dmole^{-1}$, n is the number of amino acids in the polypeptide chain, m° is the measured ellipticity, and l is the path length in centimeters. The CD spectra were analyzed using several CD deconvolution programs (CONTIN, K2D, and others) with poor results. This is not surprising since it is well-known that the spectra from proteins rich in β sheet are difficult to analyze (for review see ref *39*). An approximate value for the percentage of β sheet in the protein was obtained using the following equation:

$$[\Theta_{\mathrm{obs,217nm}}] = f_\beta[\Theta_{\beta,\mathrm{217nm}}] + f_{\mathrm{r}}[\Theta_{\mathrm{r,217\,nm}}]$$

where $[\Theta_{\mathrm{obs,217\,nm}}]$ is the observed value at 217 nm converted to MRE as described above. $[\Theta_{\beta,\mathrm{217\,nm}}]$ and $[\Theta_{\mathrm{r,217\,nm}}]$ are the reported values for poly-L-lysine in 100% β-sheet (−18 400 deg cm^2 $dmole^{-1}$) and 100% random (+4600 deg cm^2 $dmole^{-1}$) conformations, respectively (*40*). f_β and f_{r} are the fraction of β sheet and the fraction of random conformation respectively ($f_{\mathrm{r}} = 1 - f_\beta$). The estimate assumes that the contribution from α helices is negligible. This is reasonable given the intensity and shape of the observed spectra and the predominantly β-sheet content of porins (for

example, OmpF (*2omf*) contains 5% helix as determined by crystallography).

Folding kinetics were measured by using an Aviv 62DS circular dichroism spectrometer. Detergent was manually injected with a syringe into a cuvette with stirring. Injection and mixing took <10 s. The data were fit to a single exponential using SigmaPlot 2000 (SPSS Science, Chicago, IL).

Proteolysis. Limited proteolysis was performed at room temperature. A typical reaction (10 μL) contained OmpGm (0.5 mg/mL) and proteinase K (5 μg/mL) in 10 mM Tris·Cl, pH 8.0. The reaction was allowed to proceed for 5 min and then was stopped by the addition of PMSF (10 mM final), followed by incubation for 5 min at room temperature. Samples were then mixed with loading buffer and analyzed in a 12% SDS-polyacrylamide gel.

Bilayer Recordings. Planar bilayer experiments were performed in a Teflon apparatus with a volume of 2.5 mL per chamber. The chambers were separated by a 25-μm-thick Teflon film (Goodfellow, Malvern, PA) in which a 100−150 μm hole had been made with an electrical arc. Planar bilayers were formed from 1,2-diphytanoyl-*sn*-glycero-3-phosphocholine (Avanti Polar Lipids, Birmingham, AL) dissolved in highly purified pentane (Burdick & Jackson, Allied Signal Inc., Muskegon, MI). Lipid was deposited as a monolayer on the surface of the buffer in the cis and trans chambers. The bilayer was formed by raising the level of each chamber above the orifice which had been pretreated with a hexadecane/pentane (1:10 v/v) solution (*41*). Electrodes were made by coating a silver wire with AgCl by using a 10% (v/v) solution of Clorox and then inserted into agar bridges containing 3 M KCl. The cis compartment was at ground, and a positive potential indicates a higher potential in the trans chamber. A positive current is one in which cations flow from the trans to the cis side. Chambers were filled with 10 mM Tris·HCl, pH 8.0, 1 M NaCl, unless otherwise noted. The current was amplified with a Dagan 3900A integrating patch clamp amplifier (Dagan Corp., Minneapolis, MN), filtered with a Bessel filter (model 900, Frequency Devices, Haverhill, MA) at 1000 Hz and then acquired by a personal computer (sampling at 200 μs) after digitization with a DigiData 1320A A/D board (Axon Instruments, Foster City, CA). The data were analyzed with Clampex 9.0 software (Axon Instruments).

RESULTS

OmpGm Closure at Low pH or by Covalent Modification. Many porins close spontaneously in planar bilayers under conditions of high applied potential (*18*−*21*) or low pH (*16*, *42*). Voltage gating has been shown previously to occur in a single step for OmpG, consistent with a functional monomer (*17*). In the present work, the effect of pH on OmpGm gating was investigated. In these experiments, OmpGm was incorporated into a bilayer after dilution from 1% Genapol X-080. The mechanism of transfer of the protein into the bilayer is not understood, but the functional form in the bilayer is assumed to be the fully folded form (F) described below. This supposition is based on the value of the unitary conductance (0.81 nS in 1 M NaCl, pH 7.4), which is consistent with a 14-stranded barrel, and the stability and uniformity of the pores (*17*). The pH values in the cis and trans chambers were changed from the initial value by adding 1 M sodium acetate buffer, pH 5.2, resulting in a final pH of 5.9 in both chambers. At pH 5.9, the current fluctuates rapidly reflecting open and closed states ($n = 3$, Figure 1A). Individual openings and closures were analyzed and found to occur in a single step. The lack of any substates in this transition is further demonstrated in the amplitude histogram (Figure 1B), which shows only two populations, open and closed. When the pH is lowered further to pH 4.7, OmpGm is primarily closed with short spikes to higher conductance levels. The gating behavior can be reversed by raising the pH of the chamber above pH 6 with 1 M Tris·HCl, pH 8.2. These data demonstrate that OmpGm gates reversibly near pH 6. The open probability was determined over a wide range of pH values. When the data were plotted against the pH of the solution and fit to the Henderson−Hasselbalch equation, an apparent pK_a value of 6.0 was obtained (data not shown).

An additional experiment was designed to demonstrate that a single polypeptide forms the ion-conducting channel. A single cysteine mutant of OmpGm was made, designated Gm93C (E93C). This mutation is predicted to be in the middle of the fourth transmembrane β strand (*7*, *17*). Further, residue 93 lies in the middle of a region of alternating reactive and unreactive positions as defined by cysteine-scanning mutagenesis and reaction with MePEG-OPSS, M_r 5030 Da, in detergent solution. The findings (unpublished data) are consistent with the existence of a β strand in which the residues alternately point into and out of the lumen of the barrel. A cysteine at position 93 is reactive and flanked by unreactive (detergent-embedded) residues, which indicates that residue 93 projects into the lumen of the OmpG pore. Gm93C was incorporated into planar lipid bilayers and formed channels similar to those of wild-type OmpGm. The addition of a bulky thiol-directed poly(ethylene glycol) (MePEG-OPSS, M_r 970 Da) resulted in blockade of the channel ($n = 3$, Figure 1C). The block was persistent but could be reversed by the addition of DTT ($n = 3$, Figure 1D). The covalent modification does not completely close the channel, and fluctuations between two low conductance states are seen. Both the reaction with the PEG reagent and its reversal by DTT occurred in a single step, indicating the presence of one cysteine and therefore a single polypeptide per channel.

Characterization of Water-Soluble OmpGm. OmpGm remains soluble when dialyzed from 8 M urea into Tris·HCl buffer, pH 8.0, lacking detergent and salt. OmpGm could be stored in this buffer at −80 °C at concentrations greater than 10 mg/mL. The water-soluble form of OmpGm has an apparent molecular weight, by SDS-PAGE, of 34 kDa when samples are not heated, in agreement with the calculated molecular weight (32.9 kDa). In addition, the water-soluble protein was analyzed by MALDI-TOF mass spectrometry, which gave a molecular mass of 32 930 ± 40 Da, indicating that the N-terminal Met is not removed. OmpGm, while monomeric upon SDS-PAGE, was found to form discretely sized aggregates by gel filtration (see below).

Water-soluble OmpGm binds the dye 8-anilino-1-naphthalene sulfonate (ANS) indicating the presence of a hydrophobic environment formed by the protein. In water alone, ANS is only weakly fluorescent. The binding of ANS by water-soluble OmpGm results in an 8-fold increase in

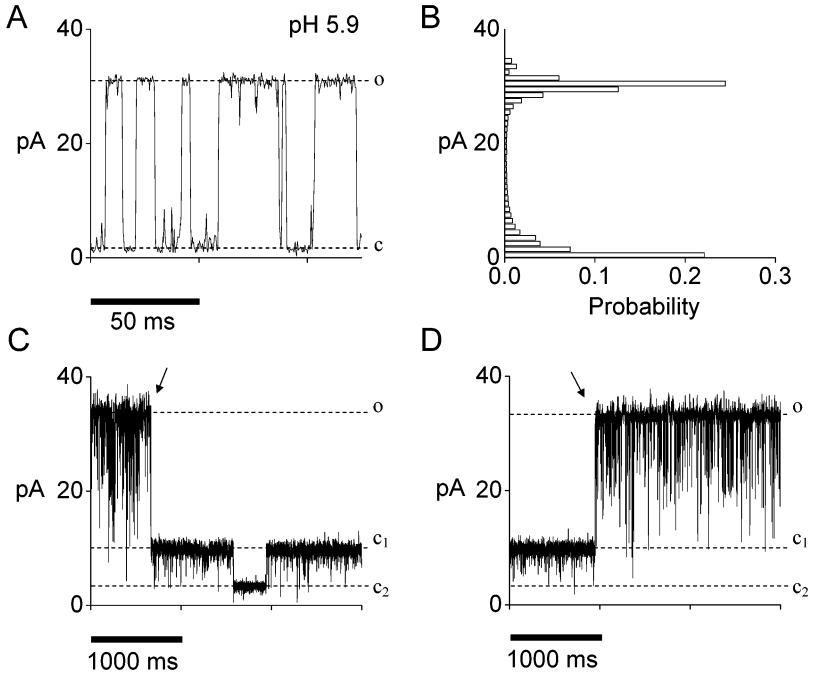

FIGURE 1: OmpGm closure by low pH or covalent modification. (A) Gating of a single OmpGm channel at pH 5.9. The (o)pen and (c)losed states are marked by dashed lines. (B) All-points amplitude histogram of OmpGm at pH 5.9; the total number of points has been normalized to 1. (C) Blockade of a single Gm93C channel after the addition of 0.5 mM MePEG-OPSS, M_r 970 Da, to the cis and trans baths. The closure is marked with an arrow. The two low conductance states (c_1 and c_2) are marked with dashed lines. (D) Reversal of Gm93C blockade after the addition of 1 mM DTT to the cis and trans baths; the opening is marked with an arrow. In all experiments, the cis and trans chambers contained 1 M NaCl, 10 mM Tris·HCl, pH 8.1. In panels A and B, there is additional 20 mM (final) sodium acetate buffer and the pH is 5.9. The transmembrane potential was +40 mV in all experiments.

the fluorescence of the dye. ANS binding by OmpGm can be abolished by denaturing the protein. A denaturation curve of OmpGm in urea was constructed by monitoring the decrease in ANS fluorescence (Figure 2A). The midpoint of the unfolding curve was 1.3 M urea. Water-soluble OmpGm was completely denatured in 4 M urea, when the ANS fluorescence was similar to that seen in 4 M urea in the absence of protein. ANS binding has been used to demonstrate the presence of a molten globule state, a compact fold possessing secondary structure but non-native tertiary structure (*43*). The molten globule state of lysozyme, for instance, binds ANS resulting in a 7-fold increase in fluorescence over the denatured state (*44*). Our data demonstrate that OmpGm can exist in a water-soluble state, possibly as a molten globule, and that this state is distinct from the denatured state.

Folding OmpGm by Direct Detergent Addition. OmpGm renaturation was originally initiated by dialysis from urea into detergent-containing buffer (*17*). In the present work, a new folding protocol was developed with water-soluble OmpGm as a starting point. Water-soluble OmpGm can be folded by the direct addition of concentrated detergent to the protein solution, resulting in a distribution of bands upon SDS-PAGE that is similar to the distribution arising from OmpGm folded by dialysis from urea into detergent. For instance, OmpGm was folded by the direct addition of 1% Genapol X-080 or dialysis from 8 M urea into 1% Genapol X-080 (12 h at 4 °C). Portions of both samples were then incubated at 0 °C, 37 °C and 50 °C for 5 h, and no differences in the amounts of heat-modifiable protein were seen when the results from the two sets of conditions were compared (data not shown). In addition, water-soluble protein folded by direct detergent addition showed protease resistance

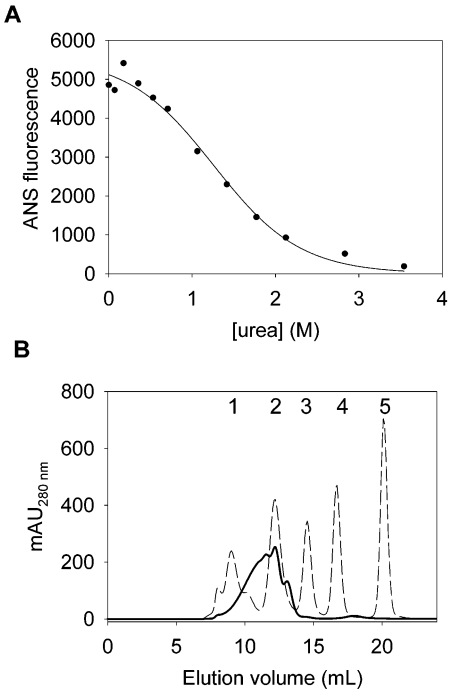

FIGURE 2: Properties of water-soluble OmpGm. (A) Denaturation of OmpGm (30 μM) in urea measured by ANS binding at 23 °C, pH 8.0. Fluorescence is in arbitrary units. (B) Gel filtration experiment comparing water-soluble OmpGm (—) with standards (---): Peak 1, thyroglobulin (670 kDa); peak 2, gamma globulin (158 kDa); peak 3, ovalbumin (44 kDa); peak 4, myoglobin (17 kDa); peak 5, vitamin B-12 (1.35 kDa).

and increased β-sheet content by circular dichroism, similar to that reported for protein folded by dialysis into detergent (*17*).

For many of the remaining experiments reported here, Genapol X-080, was replaced with *n*-octyl-β-D-glucopyranoside (OG). Genapol X-080 is not an ideal detergent for folding studies. It is difficult to remove by dialysis and commercially available Genapol X-080 contained impurities that absorbed at 280 nm. In addition, there is the potential for decomposition of this polyoxyethylene detergent into aldehydes and peroxides that can modify proteins (*45*). OG is a well-studied detergent (*46*) and is commonly used with membrane proteins, but it was not used earlier because it is prohibitively expensive as a component of dialysis buffer.

The only difference between the protein folded by direct detergent addition when compared to protein folded by dialysis was the appearance of a weak 56 kDa band upon SDS-PAGE (see below). This band was not protease-resistant and was never seen in samples folded by dialysis (*17*) or in the absence of detergent. The 56 kDa band is seen in samples incubated with both OG and Genapol X-080, demonstrating that it is not detergent-specific. One possible explanation for the 56 kDa band was that direct detergent addition stabilized a water-soluble oligomer. To address this, water-soluble OmpGm was analyzed by size exclusion chromatography in the absence of detergent. OmpGm, which was monomeric by SDS-PAGE, eluted from the column as a cluster of several peaks (Figure 2B). The elution profiles of four different batches of water-soluble OmpGm were analyzed, and all gave a similar distribution. The elution volumes of the major peaks were compared with those of gel filtration standards. On the basis of this, the three major peaks of OmpGm correspond to proteins with apparent masses of 96, 147, and 193 kDa. However, since size exclusion chromatography separates proteins based on size and shape rather than molecular mass, it is not a reliable way to estimate the number of OmpGm polypeptides in each peak. Fractions corresponding to the different peaks were analyzed a second time on the same column to determine whether the putative oligomers were in equilibrium with each other. After incubation at 23 °C for 24 h, the 193 kDa fraction did not contain an appreciable amount of the 96 or 147 kDa peaks. Likewise, the fraction containing the 147 kDa peak was analyzed a second time and did not contain an appreciable amount of the other species. These data indicate that the species seen by gel filtration are stable and not in rapid equilibrium with each other. In addition, all of the fractions collected were able to fold into a heat-modifiable species when incubated with detergent.

The properties of water-soluble OmpGm were compared to those of detergent-folded OmpGm. Exposure of water-soluble OmpGm to 5 μg/mL proteinase K for 5 min results in complete digestion of the protein. This is in contrast to the OmpGm folded by dialysis into detergent solution (*17*) or folded by direct detergent addition, where a large fraction of the protein is resistant to digestion by proteinase K. It should be noted that in detergent-folded samples, composed of a mixture of the 34 and 28 kDa forms, the 34 kDa band was always completely digested indicating that proteinase K is not inhibited by detergent at the concentrations used here. In addition, the activity of proteinase K was determined to be unaffected by the presence of detergent by using the proteinase K-sensitive staphylococcal α-hemolysin monomer as a substrate.

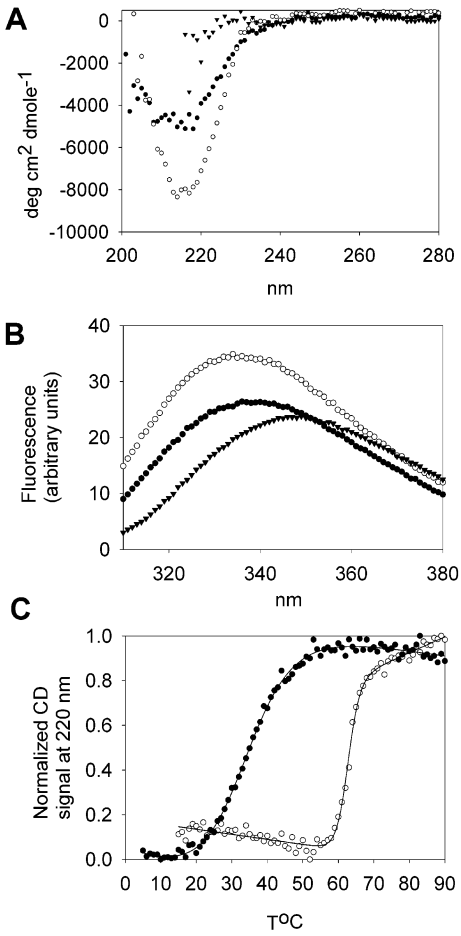

FIGURE 3: Comparison between water-soluble and detergent-folded OmpGm. All solutions were buffered with 10 mM Na phosphate, pH 8.0. (A) CD spectra of OmpGm (0.031 mg/mL) in buffer alone (●), 1% OG (○), and 8 M urea (▼). (B) Tryptophan fluorescence spectra of OmpGm under the same conditions as in panel A. (C) Thermal denaturation curves of OmpGm determined by CD in buffer alone (0.045 mg/mL OmpGm) (●) and 1% OG (0.036 mg/mL OmpGm) (○). The temperature of the cuvette was increased in 1° increments with a 5 min equilibration time at each point. Data were normalized such that the minimum value (100% folded) was 0, and the maximum value (100% unfolded) was 1. For OmpGm in buffer, "0" corresponds to −26.5 mdeg, and "1" corresponds to −17.7 mdeg. For OmpGm in 1% OG, "0" corresponds to −29.7 mdeg, and "1" corresponds to −14.2 mdeg.

The secondary structure of water-soluble OmpGm was analyzed by circular dichroism (CD) and found to have a spectrum consistent with a mixture of β sheet and random coil (Figure 3A). The water-soluble form has a 40−50% lower mean residue ellipticity at 217 nm than OmpGm in detergent solution. The mean residue ellipticity of OmpGm at 217 nm in Na phosphate buffer is -4300 ± 600 deg cm^2 dmole^{-1} (∼39% β sheet), compared to OmpGm in OG, which has a mean residue ellipticity of -7800 ± 400 deg cm^2 dmole^{-1} (∼54% β sheet). For comparison, the crystal structure of OmpF (*2omf*) shows a composition of 55% β sheet, 5% α helix, and 40% random coil.

The fluorescence of the 10 tryptophans in OmpGm was used to probe the conformation of the protein under various conditions (Figure 3B). The emission spectrum of water-soluble OmpGm (0.031 mg/mL) has $\lambda_{em} = 338$ nm, which is comparable to the value in 1% OG where $\lambda_{em} = 335$ nm. The main difference between the spectrum in buffer alone versus detergent is a 30−40% increase in the intensity in

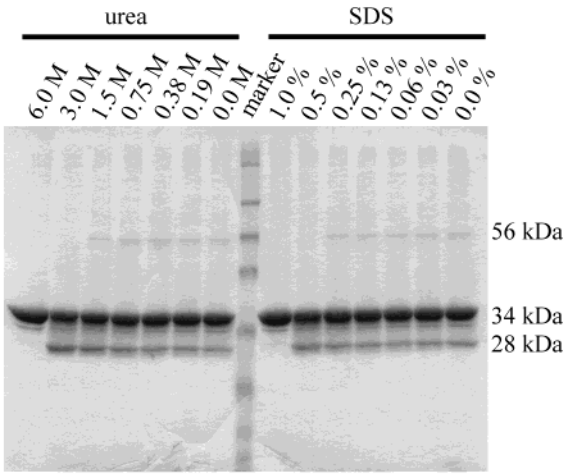

FIGURE 4: 12% SDS-PAGE showing the effect of denaturant on OmpGm folding. OmpGm was incubated for 1 h at 23 °C in 1.5% OG with various concentrations of denaturant. The samples on the left half of the gel were incubated in the presence of 6, 3, 1.5, 0.75, 0.38, 0.19, and 0 M urea. The samples on the right half of the gel were incubated in the presence of 1%, 0.5%, 0.25%, 0.13%, 0.063%, 0.031%, and 0% SDS. All solutions were buffered with 10 mM Na phosphate buffer, pH 8.0. Protein was visualized by staining with Coomassie Blue.

the presence of detergent. OmpGm in 8 M urea is red-shifted roughly 10 nm (λ_{em} = 347 nm) and has a 5−10% decrease in intensity compared to water-soluble OmpGm. The interpretation of these spectra is complicated by the large number of tryptophans contributing to the signal. In general, however, a red shift and decrease in intensity both indicate increased exposure to solvent. In this case, the tryptophans in OmpGm are the most solvent exposed in urea and the least exposed in detergent (OG).

Thermal denaturation of water-soluble OmpGm was monitored by using circular dichroism at 220 nm. A plot of fraction unfolded versus the temperature of the solution shows a sharp unfolding transition (Figure 3C). When the temperature of the cuvette was lowered to 25 °C after thermal denaturation, the CD signal did not recover, indicating that the unfolding of OmpGm in Na phosphate buffer is not reversible. The thermal denaturation curve for water-soluble OmpGm was fit using the method described by Pace and Scholtz (*47*) and gives a unfolding midpoint (T_m) of 34.1 ± 0.6 °C. The thermal denaturation of OmpGm in 1% OG also occurs in a single sharp step (Figure 3C). In contrast to the water-soluble form, OmpGm unfolding in detergent is reversible. Using the same fitting method, the T_m for OmpGm in 1% OG is 62.6 ± 0.1 °C.

Effect of Chemical Denaturants on OmpGm Folding in Detergent Solution. The absence of the 56 kDa band in protein that was folded by dialysis from denaturant into detergent raised the question of what role, if any, denaturant might play in OmpGm folding. The efficiency of folding was determined by examining heat modifiability as a function of denaturant. Water-soluble OmpGm was incubated in 1.5% OG, pH 8.0, containing urea (0−6 M) or SDS (0−1%). The folding reactions were incubated at 23 °C for 1 h and then analyzed by SDS-PAGE (Figure 4). The inclusion of 3 M urea, resulted in an increase in the amount of heat-modifiable protein and an absence of the 56 kDa form. It should be noted that in 3 M urea the water-soluble form of OmpGm is

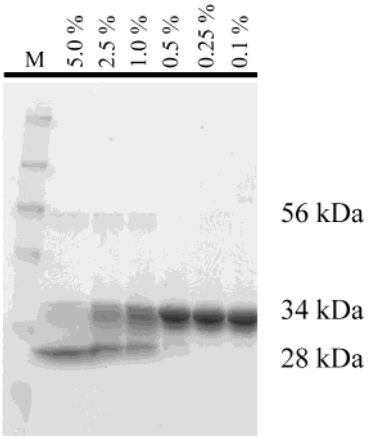

FIGURE 5: 12% SDS-PAGE showing the dependence of folding on the concentration of OG. OmpGm was folded in 5%, 2.5%, 1%, 0.5%, 0.25%, and 0.1% OG (final). All solutions were buffered with 10 mM Na phosphate buffer, pH 8.0, at 50 °C for 1 h. Protein was visualized by staining with Coomassie Blue.

unfolded, as measured by ANS fluorescence (Figure 2). In 6 M urea no heat-modifiable protein is seen. Inclusion of SDS had a similar effect, 0.5% SDS improved the overall folding yield and prevented formation of the 56 kDa form. At 1%, SDS inhibits folding, and no heat-modifiable protein is seen. These experiments show that denaturation, or partial denaturation, of the water-soluble protein promotes folding and prevents the formation of the 56 kDa form.

Determination of Optimal Folding Conditions. It was demonstrated above that the inclusion of denaturant improves the folding of OmpG and prevents the formation of the 56 kDa species. Four additional variables were examined individually in order to maximize folding. They were detergent concentration, pH, temperature, and incubation time. The detergent was considered first. Several detergents were assayed for folding activity at a concentration of 1%, which is at least twice the CMC. As measured by heat modifiability and protease resistance, Genapol X-080, Triton X-100, *n*-dodecyl-*β*-D-maltoside, Tween 20, and OG all support folding. Cholate, *n*-dodecylphosphocholine, and SDS do not support folding on their own. Of the detergents that support folding, three are polyoxyethylene based. The latter are heterogeneous in molecular mass and decompose into reactive species that can damage proteins (*45*). They are also difficult to remove by dialysis. The commonly used detergent OG, however, is an excellent detergent for membrane protein experiments and therefore it was studied in more detail.

The dependence of folding on detergent concentration was determined by incubating water-soluble OmpGm with 0.1% to 5% OG (Figure 5). OmpGm was found to fold into a heat-modifiable form at concentrations of OG above 0.5% (17 mM). This corresponds to the CMC of OG (18−20 mM in <50 mM NaCl (*46*)) and indicates a requirement for micellar rather than monomeric detergent. These experiments also demonstrated that the 56 kDa band is only formed at detergent concentrations above the CMC. As a control, the concentration dependence of folding in Genapol X-080 was also tested to ensure that the effect was not limited to OG. Folding was only seen above the CMC of Genapol X-080 (CMC 0.15 mM). Finally, while there is an apparent increase in the fraction of OmpGm that is heat-modifiable in 5% OG, the protease resistance is not improved by concentrations of

OG over 1−2% (data not shown). OG was used for the remaining experiments and was always above the CMC at >1%.

The pH dependence of OmpGm folding was determined in 1% OG at 37 °C. Several buffers were used to adjust the pH. First, a mixed buffer composed of citrate, phosphate, and borate (10 mM each) was adjusted within the range pH 4 to 11. This system was chosen because the pK_a values of the buffer components are relatively insensitive to temperature change. To ensure that the observed changes in folding efficiency were not an effect of the buffer system alone, the experiment was repeated using two other buffers, MES·NaOH below pH 7 and Tris·HCl above pH 7. For these two buffers, the pH at 37 °C was calculated by using the measured pH at 23 °C and the temperature factor for the buffer ($\Delta pK_a/\Delta T = -0.011$ for MES, $\Delta pK_a/\Delta T = -0.028$ for Tris). OmpGm folding is greatly reduced or abolished at pH values below 6. Above pH 6, the dependence of folding on pH is not strong, but there is an improvement in folding at slightly alkaline pH values (pH 7−9). For comparison, maximum folding of OmpA and OmpF was at pH 10 and pH 6.5, respectively (*48*). The efficiency of OmpA folding is almost 100% at pH 10 and is greatly reduced at lower pH values. In contrast, only 15% of OmpF is detected as folded trimers even at the optimal value of pH 6.5.

The incubation of OmpGm in detergent at elevated temperature results in an increase in the amount of heat-modifiable protein compared to incubation at 23 °C (*17*). OmpGm folding in 1% OG was measured after 1 h as a function of temperature (Figure 6A). Maximum folding was seen between 50 and 60 °C, while the 56 kDa band was most efficiently formed at 37 °C. At 55 °C, water-soluble OmpGm is completely unfolded according to the thermal denaturation data acquired by CD (Figure 3). Detergent-folded OmpGm, however, unfolds above 60 °C. Thus, the optimum folding temperature lies between these two thermal unfolding transitions. It is worth noting that the inclusion of 1.5 M urea lowers the optimum temperature from 55 to near 37 °C (data not shown).

In addition to varying the temperature, the incubation time was also considered. OmpGm was incubated in 1.5% OG at 23, 37, and 55 °C from 15 min to 5 h (Figure 6B). Samples were then loaded either directly onto an SDS-PAGE gel without heating or proteolyzed and loaded with or without heating. In Figure 6B, the first five lanes (after the marker lane) in each panel demonstrate the acquisition of heat modifiability as a function of time. The middle five lanes show that after proteolysis for 5 min in 5 μg/mL proteinase K, all of the protein in the 34 and 56 kDa bands is digested. The samples in the last five lanes were proteolyzed and heated to 95 °C in order to show how much full-length OmpGm remains after proteolysis. In all cases, longer incubation and higher temperature correlate with improved folding as monitored by heat modifiability and protease resistance. The analysis of band densities indicates that the folding as determined by SDS-PAGE occurs with a halftime of 1 h at 23 °C ($t_{1/2}$ = 40 min at 37 °C, $t_{1/2}$ = 10 min at 50 °C).

In summary, these experiments indicate that the optimal conditions for folding OmpGm are, pH 7−9 buffer containing >1% OG, and 1.5 M urea or 0.1% SDS. The optimal incubation conditions are 3 to 5 h at 37 °C. Using relatively mild conditions (4% OG, 1.5 M urea, 10 mM Na borate, pH 9.0, at 37 °C, 5 h), the majority (>90%) of the protein is converted to a heat-modifiable and protease-resistant form with no apparent off pathway aggregation (Figure 7A). Similar results were also obtained at pH 8.0. The CD spectrum of OmpGm folded under optimal conditions (4% OG, 1.5 M urea, 10 mM borate, pH 9.0, at 37 °C, 5 h) was acquired and was similar to the spectrum reported above for OmpGm in 1% OG (Figure 3A).

The effect of elevated temperature and the presence of urea on the detergent phase was also considered. The CMC

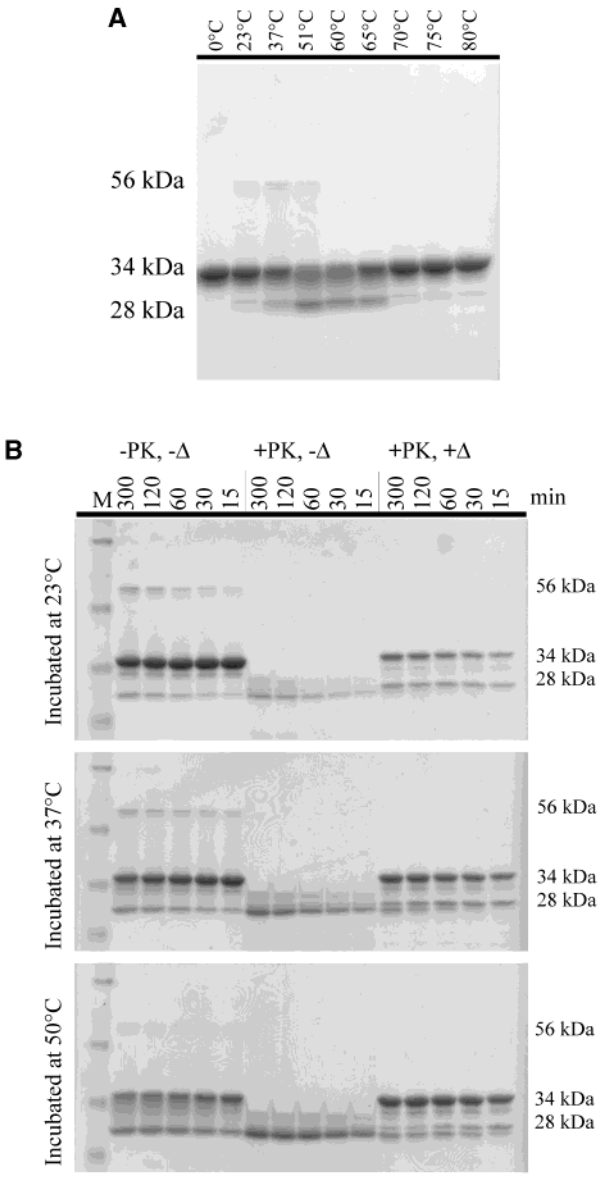

FIGURE 6: Dependence of folding on temperature and time examined by 12% SDS-PAGE. (A) Heat modifiability as a function of temperature. OmpGm was incubated in 1% OG at the indicated temperatures for 1 h. (B) Heat modifiability and protease resistance in 1.5% OG as a function of time at three temperatures. The first five lanes (after the marker lane) are OmpGm loaded without proteolysis or heating to 95 °C. In the middle five lanes, OmpGm was digested for 5 min with 5 μg/mL proteinase K (PK). In the last five lanes, OmpGm was proteolyzed and heated at 95 °C for 5 min. The incubation temperature is indicated next to each panel and incubation times are indicated above each lane. All solutions were buffered with 10 mM Na phosphate buffer, pH 8.0. Protein was visualized by staining with Coomassie Blue.

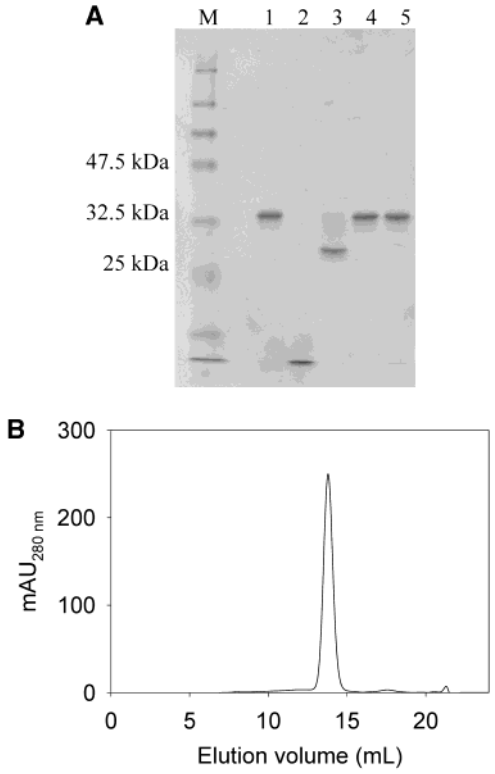

FIGURE 7: OmpGm folding under optimal conditions. (A) 12% SDS-PAGE showing OmpGm folded in 4% OG, 1.5 M urea, 10 mM borate, pH 9.0. Lane 1, water-soluble OmpGm; lane 2, water-soluble OmpGm digested for 5 min in 5 μg/mL proteinase K; lane 3, OmpGm in 4% OG, 1.5 M urea, pH 9.0 at 37 °C for 5 h; lane 4, protein from lane 3 heated to 95 °C for 5 min; lane 5, protein from lane 3 digested for 5 min in 5 μg/mL proteinase K and heated to 95 °C for 5 min. Protein was visualized by staining with Coomassie Blue. (B) Elution of OmpGm folded in 1% OG, 1.5 M urea, from a Superdex 200 HR size exclusion column equilibrated in 1% OG, 100 mM NaCl, 10 mM Na phosphate, pH 8.0.

of OG has been characterized at elevated temperatures and is found to decrease from 31 mM at 5 °C to 16 mM at 40 °C (*49*). The experiments described above were carried out in OG at a concentration of ≥1% (34 mM), which is roughly twice the CMC at 25 to 37 °C. The inclusion of 1.5 M urea in the OG solution raises the CMC from 21 mM to 26 mM at 23 °C, as measured by ANS binding. In 1% OG, the concentration of micelles is 100−200 μM, which is in excess of the protein concentration (25−50 μM) used in all experiments.

To determine how much detergent was associated with each polypeptide chain, detergent-folded OmpGm was analyzed by size exclusion chromatography in the presence of 1% OG. OmpGm folded in 1% OG with 1.5 M urea was eluted from the column as a sharp peak (Figure 7B). A comparison of the elution volume of detergent-folded OmpGm with the elution volumes of protein standards in 1% OG gives an apparent molecular weight of 75 kDa for the OmpGm−detergent complex. An OG micelle has a mass of 22 kDa (*46*), and a single OmpGm polypeptide has a mass of 32.9 kDa, giving a predicted mass of 55 kDa for a 1:1 complex. However, it is unlikely that OmpGm simply inserts into the small OG micelle (hydrodynamic radius 23Å, aggregation number = 75; ref *46*). OG in crystals of trimeric OmpF has been studied by neutron diffraction and found to form a 15 Å-wide belt around the protein composed of

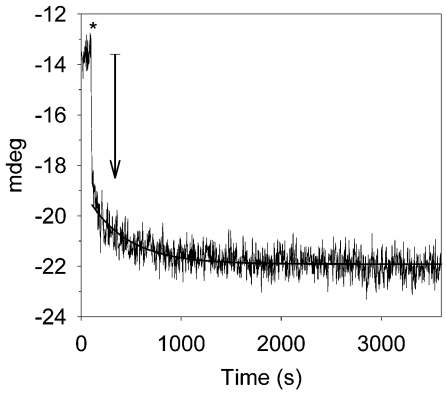

FIGURE 8: Kinetics of folding monitored by CD at 220 nm (25 °C). At 100 s (*), OG was injected into a cuvette containing OmpGm in 10 mM Na phosphate, pH 8.0, with stirring (1.5% OG final). The burst phase is indicated by the arrow. The data following the burst phase was fit to a single exponential (—).

detergent tails, which is in turn surrounded by a ∼9 Å-thick shell composed of detergent headgroups (*50*). On the basis of these findings, the 30 Å-diameter OmpGm, surrounded by a hemitoroidal (semicircular cross-section) ring of detergent 23 Å thick (minor axis), would form a complex ∼76 Å wide. A calibration curve comprising the Stokes' radius as a function of molecular mass for eight gel filtration standards was used to obtain an approximate radius for the 75 kDa OmpGm−detergent complex of 37 Å, which is in keeping with the diffraction studies on OmpF. A hemitoroid of OG surrounding OmpGm has a calculated volume of 129 000 Å^3, more than the volume of two OG micelles (each 51 000 Å^3).

Kinetics of β Sheet Formation Monitored by CD. The folding of water-soluble OmpGm in 1% OG at 25 °C was monitored by circular dichroism as a function of time. It was expected that a slow increase in β sheet would be seen at 25 °C, since heat modifiability and protease resistance were shown to develop with a $t_{1/2}$ of 1 h (Figure 5). Injection of detergent into water-soluble OmpGm, however, results in a rapid increase in β sheet, monitored at 220 nm (Figure 8). An initial burst phase, during the mixing time of the experiment, accounted for 60% ± 5% of the total signal change. The remaining data could be fit to a single exponential with $k = 0.0020 \pm 0.0004$ s^{-1} ($t_{1/2} = 390 \pm 86$ s, $n = 4$). The shortest time point reliably recorded by the gel electrophoresis experiments described earlier is 15 min. Within the first 15 min of the CD experiment, >80% of the total change in signal has occurred. SDS-PAGE, however, shows only a small amount of heat-modifiable and protease-resistant protein at this point. These data point to a rapid transformation into an intermediate enriched in β sheet that lacks heat modifiability and protease resistance. Prior to detergent addition and after the experiment was complete, CD wavelength scans were acquired. These spectra matched those shown previously for water-soluble and detergent-folded OmpGm.

Proximity of Termini, Probed by Disulfide Bond Formation. The experiments described above monitor two properties that would be expected to accompany the formation of a β barrel: heat modifiability/protease resistance and β sheet formation. These two properties develop on the hour and minute time scales, respectively. A third characteristic of β barrels is the close proximity of the N and C termini. This

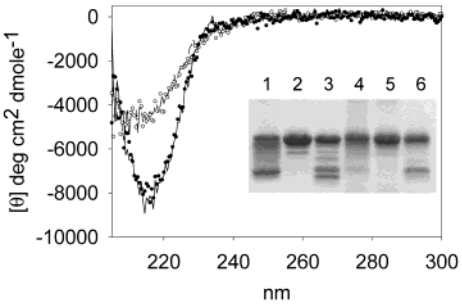

FIGURE 9: Comparison of OmpGm and Gm2C in buffer and 1% OG. CD spectra of OmpGm in buffer (---), OmpGm in 1% OG (—), Gm2C in buffer (○) and Gm2C in 1% OG (●). Inset is a 12% SDS-PAGE gel showing heat modifiability and protease resistance. Both Gm and Gm2C were folded in 1% OG at 37 °C for 3 h. Lane 1, OmpGm; lane 2, OmpGm heated at 95 °C, 5 min; lane 3, OmpGm digested with 5 μg/mL proteinase K for 5 min at 23 °C and heated to 95 °C for 5 min. Lanes 4−6: same as lanes 1−3, except Gm2C was used. All solutions were buffered with 10 mM Na phosphate buffer, pH 8.0. Protein was visualized by staining with Coomassie Blue.

is seen in the crystal structures of a number of porins (1mal, 1mpr, 1omf, 1pho, 1prn, 2por). The N-terminal nitrogen lies within 4 Å of the C-terminal carbon in the crystal structures of OmpF and PhoE. In the cases of several other porin structures, this distance is less than 20 Å.

Disulfide cross-linking has been used to demonstrate the proximity of subunits for a number of multimeric proteins including mannitol permease, the F_1F_0 ATPase and an aspartate receptor (*51*−*53*). Furthermore, engineered disulfide bonds have been used as a molecular straitjacket for a rhodopsin, to probe the folding pathway of barnase and to detect folding during the export of PhoE (*54*−*56*). To investigate the proximity of the termini in OmpG, a mutant with cysteine residues near the ends was constructed and designated Gm2C. One of the two cysteines is in the penultimate position, before the terminal phenylalanine. This position was chosen because it has been shown that the terminal phenylalanine is highly conserved among porins and is important for the proper localization, and possibly folding, of PhoE (*57*). The choice of the N-terminal position was more difficult. The N terminus of the wild-type protein is the product of processing by leader peptidase and begins with the sequence EERND. OmpGm, the pseudo wild type used in our experiments, has an N-terminal methionine and therefore begins MEERND. In Gm2C, a cysteine was added following the methionine, which resulted in the N-terminal sequence, MCEERND.

The Gm2C mutant was characterized and compared to OmpGm. Like OmpGm, Gm2C is water-soluble and has an apparent molecular weight by SDS-PAGE of 34 kDa in the presence of DTT. Gm2C does not, however, produce an appreciable amount of heat-modifiable protein compared to Gm when incubated in OG (Figure 9, compare lanes 1 and 4). Folding is, nevertheless, demonstrated by protease resistance that is similar to wild type (Figure 9, compare lanes 3 and 6). In addition, the CD spectrum of Gm2C, in both Na phosphate buffer and 1% OG, is identical to that of OmpGm under the same conditions (Figure 9). The thermal denaturation curves of Gm2C were acquired by CD in Na phosphate buffer and in 1% OG, and are similar to the curves obtained for OmpGm. Thus, with the exception of heat modifiability, Gm2C has properties similar to those of OmpGm.

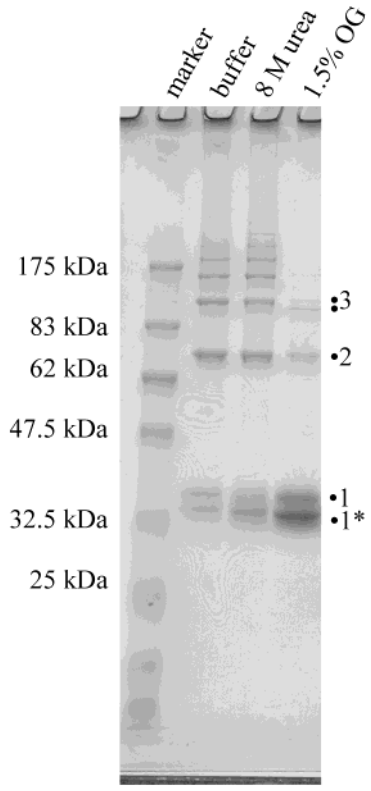

FIGURE 10: 12% SDS-PAGE showing the oxidation of Gm2C after incubation for 1 h at 50 °C under different conditions. Conditions are indicated above each lane. Oxidation was mediated by copper *o*-phenanthroline (1.3 mM). Monomeric reduced Gm2C is indicated by "1", and oxidized Gm2C is indicated by "1*". All solutions were buffered by 10 mM Na phosphate, pH 8.0. Protein was visualized by staining with Coomassie Blue.

The oxidation of the two cysteines in Gm2C to form a disulfide bond was used to demonstrate their proximity. The Gm2C mutant was reduced by the addition of excess DTT. The DTT was removed by gel filtration and the DTT-free protein was then diluted into buffer, urea or detergent. After incubation at 50°C for 1 h, the protein was rapidly oxidized by a 2-fold dilution into copper *o*-phenanthroline (1.3 mM). The oxidation reaction was allowed to proceed for five minutes, after which the reaction was quenched with EDTA and free cysteines were blocked with NEM. In buffer or 8 M urea, Gm2C formed ladders (Figure 10). These ladders extended to the top of the gel and discrete bands composed of as many as nine molecules were seen. These conditions also produced a limited amount of intramolecularly cross-linked Gm2C ($Gm2C^{ox}$), which is detected on the gel as a faster migrating species. It was confirmed that the protein in this band represents $Gm2C^{ox}$ by demonstrating that it is reduced by the addition of DTT and that it is not reactive toward the thiol-directed fluorophore Alexa 594 C_5 maleimide (data not shown). In the presence of 1.5% OG, the $Gm2C^{ox}$ species was favored, and few higher-order concatamers were seen. In some cases the higher-order bands were doublets. While the nature of these bands was not investigated, it is likely that the faster moving band in the doublet represents a circularized concatamer. These data indicate that in the detergent-folded protein the termini are close enough to preferentially form an intramolecular disulfide bond.

Table 1: Properties of OmpGm Forms

condition[a]	buffer	8 M urea	1% OG
form	W[b]	U[b]	F[b]
MW_{app}	34 kDa	34 kDa	28 kDa
protease resistance	no	n.d.	yes
CD	β (39%)	random	β (54%)
Trp λ_{max}	338 nm	347 nm	335 nm
T_m	34 °C	n.d.	63 °C
ANS binding	yes	no	n.d.
disulfide cross-link	inter-	inter-	intra-

[a] All solutions buffered with 10 mM sodium phosphate, pH 8.0. [b] W: water-soluble; U: unfolded; F: detergent-folded.

DISCUSSION

The data presented above demonstrate that OmpG is a monomeric porin. In planar lipid bilayers, the OmpGm pore closes in response to low pH. At pH 6.0 the pore alternates rapidly between open and closed states. The transition between the open and closed states occurs in a single step with no substates. If the gating event is assumed to be triggered by the protonation of a single side-chain, the pK_a of that group can be determined from the Henderson−Hasselbalch equation. The apparent pK_a is 6.0, which is the same as the pK_a of the side-chain of histidine. OmpGm has seven histidines, two of which are predicted to project into the pore (*17*). The gating of OmpF and OmpC is affected by modification with the histidine-specific reagent diethyl pyrocarbonate indicating a possible role for histidine in these cases (*58*).

In addition, a cysteine mutant of OmpG (Gm93C) was shown to be blocked after covalent modification with a bulky thiol directed reagent. The blockade occurred in a single step and was reversed in the presence of DTT. These data, combined with our previous work on voltage gating and gadolinium binding (*17*), provide convincing evidence that OmpG functions as a monomer. In addition, the gel filtration and SDS-PAGE analysis of detergent-folded OmpG presented here, combined with the initial work by Fajardo and colleagues (*7*) and a 6 Å projection structure (*22*), demonstrate that OmpG is structurally a monomer. To our knowledge, no other porin has been demonstrated this rigorously to exist and function as a monomer.

The biochemical analysis presented here characterizes several forms of OmpG (Table 1) and provides insight into the folding mechanism of the protein. We have shown that OmpGm can exist in a water-soluble form. It is unclear whether this form lies on the export and folding pathway of OmpG in *E. coli*. The mechanism by which porins are targeted to the outer membrane has been studied in some detail (for review, see refs *59* and *60*). While OmpGm is water-soluble, it does form oligomers in solution, which is most likely due either to the amphipathic nature of the β sheets that ultimately form the barrel or to hydrogen-bonding between edges of the sheets. The significance of the oligomers was not investigated here, but it is possible that they would be prevented from forming in vivo by association with periplasmic (*61*) or outer membrane (*62*) chaperones.

The water-soluble form of OmpGm is distinct from both the unfolded state in 8 M urea and the detergent-folded form. In contrast to the unfolded protein, water-soluble OmpGm binds ANS and has secondary structure as determined by CD. ANS binding may be due to the presence of a hydrophobic core region, such as that of a molten globule, or it could occur at the interfaces between oligomers. The CD data indicate that roughly 40% of the residues in the water-soluble form are in a β-sheet conformation compared to 55% in the detergent-folded form. Also, the water-soluble protein lacks the stable tertiary structure of the detergent-folded form as indicated by a lack of heat modifiability and sensitivity to proteolysis. These data indicate that the water-soluble form of OmpGm is distinct from both the unfolded and fully folded forms, and possibly resembles a molten globule.

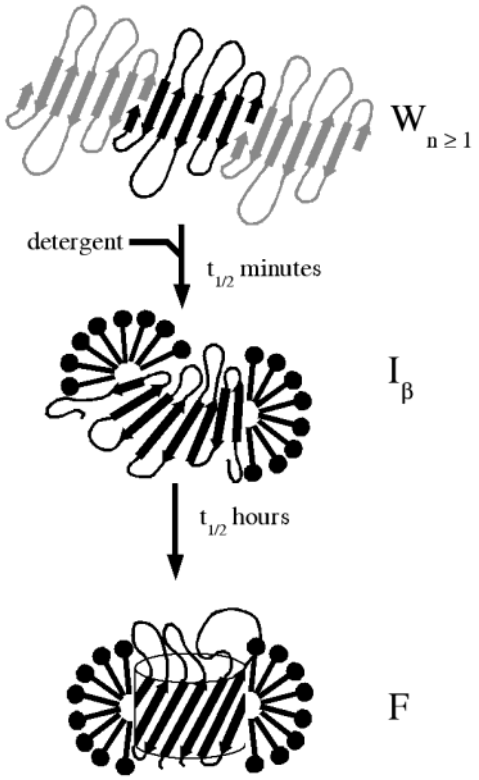

FIGURE 11: Schematic of the folding pathway for OmpGm. Three forms are shown: the water-soluble form (W), a β-sheet-rich intermediate (I_β), and the fully folded form (F).

Water-soluble OmpGm can be converted to a β-sheet rich, heat-modifiable, protease-resistant form by incubation with detergent. This conversion requires micellar detergent, in agreement with work on OmpA folding (*63*). The folding pathway can be divided into two phases (Figure 11), a fast conversion from the water-soluble protein (W) into a β-sheet rich intermediate (I_β) followed by a slow acquisition of heat modifiability and protease resistance in the final folded form (F). The transformation into a β-sheet rich intermediate itself occurs in two phases. The first phase accounts for 60% of the total increase in β sheet and happens during the dead time of the experiment <10 s. The second phase occurs with a halftime of $\sim$6 min. This transformation does not result in a significant fraction of the protein becoming heat modifiable or protease resistant.

Size exclusion chromatography demonstrates that the oligomeric water-soluble protein becomes a single species (75 kDa) when folded in OG, regardless of the band distribution by SDS-PAGE. In other words, even though detergent-folded OmpGm is often a mixture of species by SDS-PAGE, the gel filtration data do not support the presence of several species with a distribution of sizes, as

seen in the water-soluble form. The simplest interpretation of the Stokes' radius of the OmpGm-detergent complex, as determined by size exclusion chromatography, is that a single OmpGm polypeptide is associated with a detergent torus. A similar elution profile was observed when OmpGm was examined by size exclusion chromatography immediately after the addition of OG (data not shown). This result suggests that the oligomers in the water-soluble form dissociate rapidly and that the intermediate I_β associates with a substantial mass of detergent before the acquisition of heat modifiability and protease resistance. By analogy with the folding pathway of OmpA (*64*), we suggest that the I_β form of OmpG, which forms in minutes and has considerable secondary structure but is not protease-resistant or heat-modifiable, is a folding intermediate that is associated with detergent, in this case more than a single micelle, as judged by the elution volume.

Incubation of I_β in detergent for additional time (>1 h) results in little change in β-sheet content, but it is accompanied by the acquisition of heat modifiability and protease resistance, resulting in the formation of the folded form (F). These characteristics appear with a halftime of 1 h at 23 °C. Protease resistance has been proposed as a general indicator of protein folding (*65*). In the case of OmpG, the origin of protease resistance is likely two-fold: the formation of compact tertiary structure and the protection of protease-sensitive regions by the detergent torus. A number of OMPs have been demonstrated to be protease-resistant when fully assembled into membranes including OmpA, OmpF, and PhoE (*9*, *11*, *48*).

Heat modifiability reflects the inability of SDS to completely denature a protein in the absence of heating. The mechanism underlying heat modifiability is not well understood, but in OmpG it appears synchronously with the formation of tertiary structure. Heat modifiability has previously been used as a indicator of the final folded state for a number of β-barrel proteins, notably OmpA (*8*). PhoE has also been demonstrated to possess a heat-modifiable monomeric form that is thought to be an intermediate in the assembly of the trimer (*9*). Folding in OG most likely facilitates the acquisition of heat modifiability in two ways. First, as a folding substrate, the micellar surface may catalyze the formation of the β barrel, perhaps at the interfacial region between the aqueous phase and the hydrophobic core (*63*). Second, in the case of OmpGm, the detergent also serves to dissociate the water-soluble oligomers. As the barrel forms, there must be compensatory changes in the state of the detergent as it forms a toroidal structure (*50*, *66*, *67*). The closed nature of the β barrel with its full complement of hydrogen bonds renders the structure stable to denaturation.

Excess detergent, such that micelles greatly outnumber protein molecules, results in an apparent increase in heat-modifiable protein. One explanation is that excess OG (at 3−5%) forms mixed micelles with the 2.3% SDS in the gel electrophoresis loading buffer, thereby diminishing the denaturing power of the SDS. This possibility is supported by the observation that protease resistance is unaffected by high concentrations of OG. Furthermore, reduction of the SDS concentration in the loading buffer results in an increase in the amount of heat-modifiable protein. Therefore, heat modifiability should only be considered a qualitative marker, which will most often result in an underestimate of folding.

The folding pathway for OmpGm (Figure 11) is in general agreement with the data available for other OMPs. OmpA has been particularly well studied and is a good model for transmembrane β-barrel formation (*11*, *64*, *68*−*71*). OmpA collapses into a water-soluble intermediate after the removal of denaturant. In the presence of lipid bilayers, the water-soluble form of OmpA binds rapidly to the membrane surface to form the intermediate I_{M1}. Once adsorbed, OmpA inserts via at least two additional intermediates, a molten disk (I_{M2}) and a molten globule (I_{M3}). These intermediates are already rich in β structure. I_{M1} formation occurs on the time scale of minutes, with the later events occurring on the time scale of hours in the case of small unilamellar vesicles, but more quickly in detergent (*63*) or with large unilamellar vesicles comprising short-chain lipids (*71*). By analogy with OmpA, we propose that water-soluble OmpG assumes an incompletely folded, possibly molten globule, state (I_β), comprising detergent-associated β sheet. I_β then acquires heat modifiability and protease resistance, a process which takes hours in this case even in detergent. A similar folding pathway has been described for the early events in OmpF folding (*48*). While the final form of OmpF is a trimer, folding occurs via a partially folded membrane-bound monomer which may be analogous to the I_β form of OmpG.

We have shown that under optimal conditions it is possible to produce a nearly homogeneous population of OmpGm molecules that exhibit heat modifiability, protease resistance and β-sheet content comparable to native porins. OmpG is, therefore, a promising candidate for structural studies, particularly NMR, which has recently been used to solve the structures of OmpA and OmpX in detergent (*72*−*74*). In contrast to soluble proteins, relatively few membrane protein structures have been solved at high resolution. This is particularly true for NMR spectroscopy, because protein−detergent complexes are typically 50 kDa or larger. OmpA and OmpX have less than 200 amino acids each, making them the smallest transmembrane β barrels. The fact that OmpG is a monomer and can be folded efficiently in vitro makes this 280 amino acid protein a logical target for structural studies.

By far the most important factor in achieving high folding yields was the inclusion of a low concentration of denaturant. The effect of denaturant on folding has several possible explanations. For example, it might cause dissociation of the water-soluble oligomers. Since gel filtration of the detergent-folded protein in the absence of urea suggests that there is a single polypeptide in each detergent complex, the water-soluble oligomers must dissociate during folding. It is also possible that the OmpG polypeptides are partially and transiently unfolded by the denaturant.

In addition to using circular dichroism and SDS-PAGE to monitor OmpGm folding, we have also introduced a new method for monitoring β-barrel formation. The N and C termini in folded proteins are often in close proximity. This is particularly true of β barrels and has been exploited for OmpA in the form of functional circularly permuted variants (*75*). An examination of several porin crystal structures revealed that the N and C termini were less than 20 Å apart and in some cases as close as 4 Å. By using a mutant OmpGm with a cysteine residue near each end, we have shown that conditions that promote folding of OmpGm (1% OG) also result in preferential cross-linking of the termini

within a single polypeptide chain. This is in contrast to OmpGm in buffer or 8 M urea, where cross-linking is primarily intermolecular, resulting in ladders. In summary, after treatment with detergent, OmpGm displays heat modifiability, protease resistance, and high β-sheet content, as well as N- and C-terminus proximity, all hallmarks of a correctly folded β barrel.

ACKNOWLEDGMENT

We thank Dr. J. Martin Scholtz and Jason P. Schmittschmitt for their valuable input.

REFERENCES

1. Nikaido, H. (1999) *J. Bacteriol. 181*, 4−8.
2. Jap, B. K., and Walian, P. J. (1996) *Physiol. Rev. 76*, 1073−1088.
3. Nikaido, H. (1994) *J. Biol. Chem. 269*, 3905−3908.
4. Klebba, P. E., and Newton, S. M. C. (1998) *Curr. Opin. Microbiol. 1*, 238−248.
5. Schirmer, T. (1998) *J. Struct. Biol. 121*, 101−109.
6. Misra, R., and Benson, S. A. (1989) *J. Bacteriol. 171*, 4105−4111.
7. Fajardo, D. A., Cheung, J., Ito, C., Sugawara, E., Nikaido, H., and Misra, R. (1998) *J. Bacteriol. 180*, 4452−4459.
8. Beher, M. G., Schnaitman, C. A., and Pugsley, A. P. (1980) *J. Bacteriol. 143*, 906−913.
9. Jansen, C., Heutink, M., Tommassen, J., and de Cock, H. (2000) *Eur. J. Biochem. 267*, 3792−3800.
10. Dornmair, K., Kiefer, H., and Jahnig, F. (1990) *J. Biol. Chem. 265*, 18907−18911.
11. Surrey, T., and Jahnig, F. (1995) *J. Biol. Chem. 270*, 28199−28203.
12. Rosenbusch, J. P. (1974) *J. Biol. Chem. 249*, 8019−8029.
13. Cowan, S. W., Garavito, R. M., Jansonius, J. N., Jenkins, J. A., Karlsson, R., Konig, N., Pai, E. F., Pauptit, R. A., Rizkallah, P. J., Rosenbusch, J. P., and (1995) *Structure 3*, 1041−1050.
14. Hoenger, A., Pages, J. M., Fourel, D., and Engel, A. (1993) *J. Mol. Biol. 233*, 400−413.
15. Schabert, F. A., Henn, C., and Engel, A. (1995) *Science 268*, 92−94.
16. Muller, D. J., and Engel, A. (1999) *J. Mol. Biol. 285*, 1347−1351.
17. Conlan, S., Zhang, Y., Cheley, S., and Bayley, H. (2000) *Biochemistry 39*, 11845−11854.
18. Buehler, L. K., Kusumoto, S., Zhang, H., and Rosenbusch, J. P. (1991) *J. Biol. Chem. 266*, 24446−24450.
19. Wiese, A., Schroder, G., Brandenburg, K., Hirsch, A., Welte, W., and Seydel, U. (1994) *Biochim. Biophys. Acta 1190*, 231−242.
20. Song, J., Minetti, C. A., Blake, M. S., and Colombini, M. (1998) *Biochim. Biophys. Acta 1370*, 289−298.
21. Bishop, N. D., and Lea, E. J. A. (1994) *FEBS Lett. 349*, 69−74.
22. Behlau, M., Mills, D. J., Quader, H., Kuhlbrandt, W., and Vonck, J. (2001) *J. Mol. Biol. 305*, 71−77.
23. Walker, B., Kasianowicz, J., Krishnasastry, M., and Bayley, H. (1994) *Protein Eng. 7*, 655−662.
24. Walker, B., and Bayley, H. (1994) *Protein Eng. 7*, 91−97.
25. Cheley, S., Braha, O., Lu, X., Conlan, S., and Bayley, H. (1999) *Protein Sci. 8*, 1257−1267.
26. Bayley, H. (1994) *J. Cell. Biochem. 56*, 177−182.
27. Braha, O., Walker, B., Cheley, S., Kasianowicz, J. J., Song, L., Gouaux, J. E., and Bayley, H. (1997) *Chem. Biol. 4*, 497−505.
28. Saxena, K., Drosou, V., Maier, E., Benz, R., and Ludwig, B. (1999) *Biochemistry 38*, 2206−2212.
29. Lou, K. L., Saint, N., Prilipov, A., Rummel, G., Benson, S. A., Rosenbusch, J. P., and Schirmer, T. (1996) *J. Biol. Chem. 271*, 20669−20675.
30. Saint, N., Lou, K. L., Widmer, C., Luckey, M., Schirmer, T., and Rosenbusch, J. P. (1996) *J. Biol. Chem. 271*, 20676−20680.
31. Bannwarth, M., and Schulz, G. E. (2002) *Protein Eng. 15*, 799−804.
32. Gouaux, J. E., Braha, O., Hobaugh, M. R., Song, L., Cheley, S., Shustak, C., and Bayley, H. (1994) *Proc. Natl. Acad. Sci. U.S.A. 91*, 12828−12831.
33. Miles, G., Bayley, H., and Cheley, S. (2002) *Protein Sci. 11*, 1813−1824.
34. Cheley, S., Malghani, M. S., Song, L., Hobaugh, M., Gouaux, J. E., Yang, J., and Bayley, H. (1997) *Protein Eng. 10*, 1433−1443.
35. Howorka, S., and Bayley, H. (1998) *Biotechniques 25*, 765−772.
36. Studier, F. W., Rosenberg, A. H., Dunn, J. J., and Dubendorff, J. W. (1990) *Methods Enzymol. 185*, 60−89.
37. Pace, C. N., Vajdos, F., Fee, L., Grimsley, G., and Gray, T. (1995) *Protein Sci. 4*, 2411−2423.
38. De Vendittis, E., Palumbo, G., Parlato, G., and Bocchini, V. (1981) *Anal. Biochem. 115*, 278−286.
39. Greenfield, N. J. (1996) *Anal. Biochem. 235*, 1−10.
40. Greenfield, N., and Fasman, G. D. (1969) *Biochemistry 8*, 4108−4116.
41. Montal, M., and Mueller, P. (1972) *Proc. Natl. Acad. Sci. U.S.A. 69*, 3561−3566.
42. Todt, J. C., Rocque, W. J., and McGroarty, E. J. (1992) *Biochemistry 31*, 10471−10478.
43. Semisotnov, G. V., Rodionova, N. A., Razgulyaev, O. I., Uversky, V. N., Gripas', A. F., and Gilmanshin, R. I. (1991) *Biopolymers 31*, 119−128.
44. Koshiba, T., Yao, M., Kobashigawa, Y., Demura, M., Nakagawa, A., Tanaka, I., Kuwajima, K., and Nitta, K. (2000) *Biochemistry 39*, 3248−3257.
45. Ray, W. J., Jr., and Puvathingal, J. M. (1985) *Anal. Biochem. 146*, 307−312.
46. Lorber, B., Bishop, J. B., and DeLucas, L. J. (1990) *Biochim. Biophys. Acta 1023*, 254−265.
47. Pace, C. N., and Scholtz, M. (1997) in *Protein Structure: A Practical Approach* (Creighton, T. E., Ed.) pp 299−321, Oxford University Press, New York.
48. Surrey, T., Schmid, A., and Jahnig, F. (1996) *Biochemistry 35*, 2283−2288.
49. da Graca, M. M., Eidelman, O., Ollivon, M., and Walter, A. (1989) *Biochemistry 28*, 8921−8928.
50. Pebay-Peyroula, E., Garavito, R. M., Rosenbusch, J. P., Zulauf, M., and Timmins, P. A. (1995) *Structure 3*, 1051−1059.
51. van Montfort, B. A., Schuurman-Wolters, G. K., Duurkens, R. H., Mensen, R., Poolman, B., and Robillard, G. T. (2001) *J. Biol. Chem. 276*, 12756−12763.
52. Jones, P. C., Jiang, W., and Fillingame, R. H. (1998) *J. Biol. Chem. 273*, 17178−17185.
53. Chervitz, S. A., and Falke, J. J. (1995) *J. Biol. Chem. 270*, 24043−24053.
54. Struthers, M., Yu, H., and Oprian, D. D. (2000) *Biochemistry 39*, 7938−7942.
55. Clarke, J., and Fersht, A. R. (1993) *Biochemistry 32*, 4322−4329.
56. Eppens, E. F., Nouwen, N., and Tommassen, J. (1997) *EMBO J. 16*, 4295−4301.
57. Struyve, M., Moons, M., and Tommassen, J. (1991) *J. Mol. Biol. 218*, 141−148.
58. Todt, J. C., and McGroarty, E. J. (1992) *Biochemistry 31*, 10479−10482.
59. Bernstein, H. D. (2000) *Curr. Opin. Microbiol. 3*, 203−209.
60. Economou, A. (1999) *Trends Microbiol. 7*, 315−320.
61. Bulieris, P. V., Behrens, S., Holst, O., and Kleinschmidt, J. H. (2003) *J. Biol. Chem. 278*, 9092−9099.
62. Voulhoux, R., Bos, M. P., Geurtsen, J., Mols, M., and Tommassen, J. (2003) *Science 299*, 262−265.
63. Kleinschmidt, J. H., Wiener, M. C., and Tamm, L. K. (1999) *Protein Sci. 8*, 2065−2071.
64. Kleinschmidt, J. H., den Blaauwen, T., Driessen, A. J., and Tamm, L. K. (1999) *Biochemistry 38*, 5006−5016.
65. Heiring, C., and Muller, Y. A. (2001) *Protein Eng. 14*, 183−188.
66. Roth, M., Arnoux, B., Ducruix, A., and Reiss-Husson, F. (1991) *Biochemistry 30*, 9403−9413.
67. Fernandez, C., Hilty, C., Wider, G., and Wuthrich, K. (2002) *Proc. Natl. Acad. Sci. U.S.A. 99*, 13533−13537.
68. Rodionova, N. A., Tatulian, S. A., Surrey, T., Jahnig, F., and Tamm, L. K. (1995) *Biochemistry 34*, 1921−1929.
69. Kleinschmidt, J. H., and Tamm, L. K. (1996) *Biochemistry 35*, 12993−13000.
70. Kleinschmidt, J. H., and Tamm, L. K. (1999) *Biochemistry 38*, 4996−5005.
71. Kleinschmidt, J. H., and Tamm, L. K. (2002) *J. Mol. Biol. 324*, 319−330.
72. Arora, A., Abildgaard, F., Bushweller, J. H., and Tamm, L. K. (2001) *Nat. Struct. Biol. 8*, 334−338.
73. Fernandez, C., Adeishvili, K., and Wuthrich, K. (2001) *Proc. Natl. Acad. Sci. U.S.A. 98*, 2358−2363.
74. Fernandez, C., Hilty, C., Bonjour, S., Adeishvili, K., Pervushin, K., and Wuthrich, K. (2001) *FEBS Lett. 504*, 173−178.
75. Koebnik, R., and Kramer, L. (1995) *J. Mol. Biol. 250*, 617−626.

BI0344228